EUROPEAN
NETWORK

MAX-PLANCK-GESELLSCHAFT

The soft X-ray properties and the VLBI properties of AGN from the CJF sample

A search for correlations

S. Britzen[1,2], W. Brinkmann[3], R. C. Vermeulen[4], M. Gliozzi[3], R. M. Campbell[5], G. B. Taylor[6], I. W. A. Browne[7], P. N. Wilkinson[7], T. J. Pearson[8], and A. C. S. Readhead[8]

[1] Landessternwarte, Königstuhl, 69 117 Heidelberg, Germany
[2] Max–Planck–Institut für Radioastronomie, Auf dem Hügel 69, 53 121 Bonn, Germany
[3] Max–Planck–Institut für extraterrestrische Physik, Giessenbachstrasse, D-85740 Garching, Germany
[4] Netherlands Foundation for Research in Astronomy, P.O. Box 2, NL-7990 AA Dwingeloo, The Netherlands
[5] Joint Institute for VLBI in Europe, Oude Hoogeveensedijk 4, NL-7991 PD Dwingeloo, The Netherlands
[6] National Radio Astronomy Observatory, P.O. Box O, Socorro, NM 87801
[7] Nuffield Radio Astronomy Laboratories, Jodrell Bank, Macclesfield, Cheshire SK11 9DL, England UK
[8] California Institute of Technology, Department of Astronomy, 105-24, Pasadena, CA 91125

Abstract. All 293 AGN of the most recently completed VLBI survey of the Caltech-Jodrell Bank flat spectrum sample (hereafter CJF) have been observed in the ROSAT All-Sky survey and in part in pointed PSPC observations. We here summarize the radio properties, the soft X-ray properties for the complete CJF survey, and give a progress report on the search for correlations between the X-ray and VLBI properties for those sources with motion information (242 sources). Comparing the observed and the predicted X-ray flux by assuming the observed X-rays to be of inverse Compton origin, we compute the beaming or Doppler factor δ_{IC} for the CJF sources. We compare the Doppler factors with other beaming indicators derived from the VLBI observations, such as the value of the expansion velocity. In addition, we discuss a possible correlation between the complexity of the extended emission seen with the VLA (literature) and the X-ray flux density.

AGN are our principal probes of the universe on large scales; understanding them is essential to studying the evolution of the universe. The most promising tool we have is the investigation of correlations between the flux-density in different wavelength regimes and the morphological variations of the jet obtained from VLBI observations. We here present first results of the analysis of the completed survey and wish to refer to the specific papers for a detailed description of the analysis and results presented here only in summary.

1. Introduction

The CJF is unique in the combination of data quality, number of epochs, source number and homogeneity of the performed observations and data analysis. We are confident that the analysis of this complete survey will yield meaningful information on:
- the superluminal motion statistics for a complete sample of 293 AGN (see section 4.1 and Britzen et al. 2002a)
- the curvature of the pc-scale jet (see section 4.2) and jet component paths (bending, multiple paths) as a function of AGN class
- a possible evolution with redshift (first results in Britzen 2002)
- the validity of the beaming hypothesis (see section 5.1)
- a possible correlation between X-ray prominence and radio properties (this paper section 5.2 and Britzen et al. 2002b)

Future projects include the investigation of a possible correlation between radio-, optical-, and gamma-ray flux-density variability and the radio properties.

It is generally accepted that jets are the sites where the radio- to gamma-ray emission is produced. However, the details of the gamma-ray production are yet unknown and subject of debate. Two independent sources of information might help us to understand the underlying physics. Multi-wavelength flux-density campaigns of a large number of AGN are as badly needed as is detailed morphological information on the evolution of a large number of AGN jets. Combining this information is a promising tool on the way to a possible discrimination between the various high energy radiation processes.

In Fig. 1 we present the distribution of CJF sources over redshift, separated by whether they were detected by ROSAT or not.

2. CJF observations

The most recently completed CJF has been defined by Taylor et al. (1996) as a complete flux-limited sample of 293 flat-spectrum radio sources, drawn from the 6 cm and 20 cm Green Bank Surveys (Gregory & Condon 1991; White & Becker 1992) with selection criteria as follows: $S(6 \text{ cm}) \geq 350$ mJy, $\alpha_{20}^{6} \geq -0.5$, $\delta(1950) \geq 35°$, and $|b^{II}| \geq 10°$. This sample is based on the 6 cm MPI-NRAO 5 GHz surveys (Kühr et al. 1981). Optical identifications
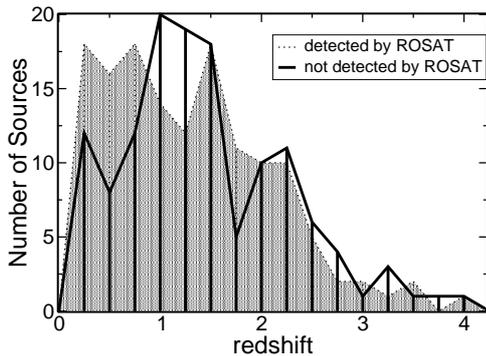
Fig. 1. The distribution of the ROSAT detected and non-detected CJF sources as function of redshift.

have been made for 97% of the CJF sample, and redshifts obtained for 92% of the objects (e.g., Stickel & Kühr 1994; Stickel et al. 1994; Xu et al. 1994; Vermeulen & Taylor 1995; Vermeulen et al. 1996).

The radio observations were performed at 5 GHz in several runs in either global-VLBI or VLBA-snapshot observations between March 1990 and November 2000. These observations are now complete; the last epoch, for a subsample of 34 sources, has been obtained in December 2000. All sources and epochs have been fully analyzed in the same standardized way; details concerning the data analysis can be found in Britzen et al. (2002a).

3. ROSAT observations

For each of the sample sources a $1° \times 1°$ field centered on the radio position was extracted from the ROSAT All-Sky Survey (RASS) and analyzed using a procedure based on standard routines within the EXSAS environment (Zimmermann et al. 1994). This procedure uses a maximum-likelihood source detection algorithm (Cruddace et al. 1988). We considered a radio source to be detected in X-rays if the likelihood of existence is greater than 5.91, which corresponds to 3σ. If no X-ray source is detected above the specified significance level, we determined the 2σ upper limit on the number of X-ray photons. To calculate the corresponding count rates we used the vignetting-corrected RASS exposure averaged over a circle with radius 5 arcmin centered on the radio position. Several of the sources, mostly the prominent objects of the sample, had been targets of pointed observations. The pointed observations are of superior statistical significance and have been used for these sources. A detailed description of the ROSAT data analysis is going to be presented in Britzen et al. (2002b). In total we have 188 quasars, of which 87 were not detected in the survey; 59 galaxies (including Seyferts), of which 37 were undetected; 43 BL Lacs (8 non-detections); and 9 objects which have not yet been classified. The highest rate of non-detection is

amongst the galaxies, whereas most of the BL Lacs have been found as strong X-ray emitters.

4. Radio properties of the CJF sources

4.1. Superluminal motion statistics

Our results presented here are based on the analysis of 402 jet component motions determined for 177 quasars, 107 for 40 galaxies, 58 for 23 BL Lac objects, and 30 for 12 still unclassified sources. 41 sources can not be included into the analysis presented here, since they either have no redshift yet, were too faint in the observations, or clearly need another epoch to clarify jet component motion. Only in rare cases is **one single** motion value representative for jet component motion in a given source; in general, a broad range of velocities can be measured. The extracted values (based on three or four snapshot observations) can not cover the complete history of jet component motion, but can reproduce the motion of the brightest and dominant jet components. In many cases brightening or dimming of the jet components and/or the reference component (the "core") from one epoch to another complicates the assignment of component identities. We find that the internal proper motions cover a wide range of positive and negative values. The most important scenarios that lead to negative values include true "backwards" motion, blending effects between components, and mis-identifications of the core (sources like 4C39.25 where the brightest component is not the core).

Despite the large spread in the data, quasars and BL Lac objects show a tendency to have the highest proper motions, 0.053 ± 0.089 mas/year and 0.053 ± 0.065 mas/year respectively, and the galaxies the slowest proper motions, 0.035 ± 0.058 mas/year. The unclassified subgroup that most likely consists of quasars reveals fast proper motions, 0.067 ± 0.098 mas/year. (Note that values quoted throughout this paper to describe a parameter associated with a class of objects represent the mean $\pm$ the standard deviation of the distribution of the parameter over all members of the class.)

The apparent velocities have been calculated from the observed proper motions using $H_0 = 65$ km s^{-1} Mpc^{-1} and a deceleration parameter of $q_0 = 0.5$. Quasars reveal the highest β_{app} (2.89 ± 4.19), the galaxies show the lowest values (0.81 ± 1.58), and the BL Lac objects have values in between (1.36 ± 1.80). We investigated the β_{app}-redshift relation for only the brightest jet component as well. The brightest component should be the maximally beamed component in a jet and can yield some representative value for motion in a given source. In addition, the brightest component can be determined with higher accuracy and traced more reliably across the epochs. Again the quasar population exhibits the highest values (2.95 ± 3.90), the galaxies reveal significantly slower motion (1.28 ± 1.62), but even slower are the BL Lacs (1.22 ± 1.45). The unclassified objects again show values indicating that this group consists of a mix of the other populations (2.00 ± 3.27).
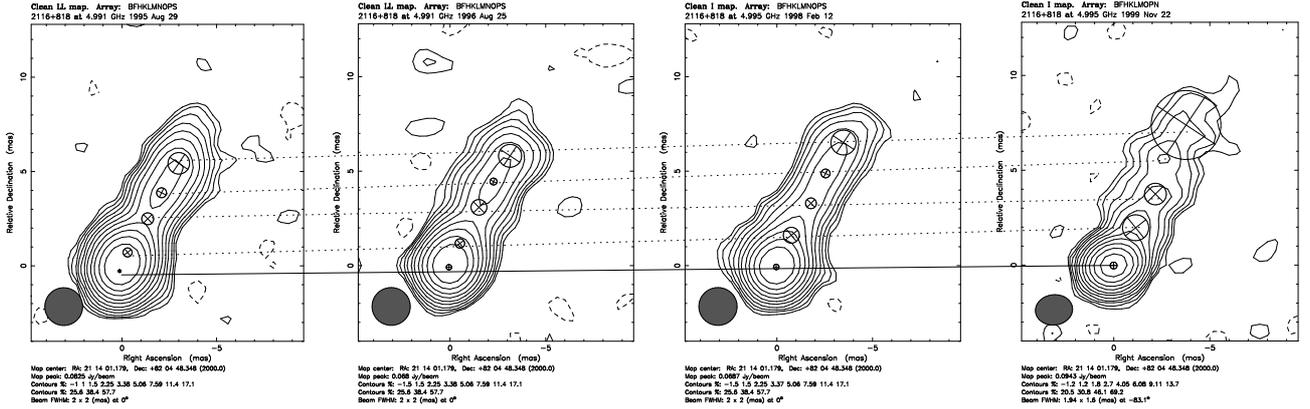
Fig. 2. An example for the rare "straight jets" in the CJF. The reference point (presumably the core) is marked by a solid line. The individual circular jet component positions and sizes are indicated in this and the following figure by encircled crosses, followed across the epochs by dotted lines. Four epochs of the quasar 2116+818 are shown.
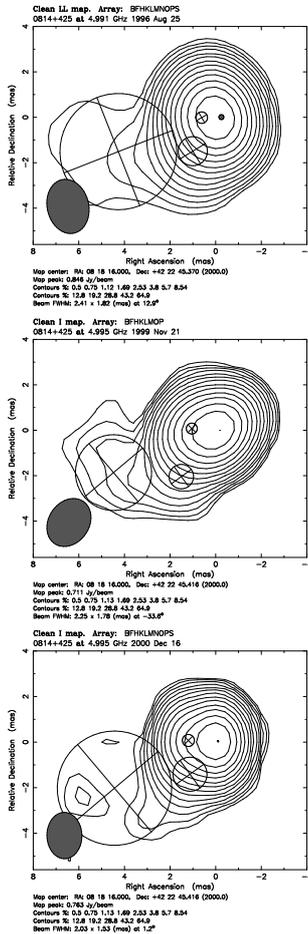

Fig. 3. An example for jet component motion in BL Lac objects: three epochs of 0814+425.

Interestingly, the brightest galaxy components move faster than the less bright galaxy components.

4.2. Parsec-scale Jet Curvature

Straight jets like in 2116+818 (Fig.2) appear to be rare cases within the CJF. Most sources reveal curved jet structures, whereby different forms of curvature occur. Especially the BL Lac objects show quite strongly bent jet paths (see the BL Lac object 0814+425 in Fig.3). Jet components in these sources move on curved trajectories with significantly changing position angle from epoch to epoch, indicating that jet components might move on helical trajectories. Several BL Lac sources show this sort of behavior, and this is reflected in a tendency towards higher values for the observed pc-scale curvature (determined from smallest and largest value for position angle observed). The mean value for this curvature is $26°\pm23°$ for the quasars and $37°\pm26°$ for the BL Lac objects.

4.3. Flux-density variability of core and jet

The vast majority of the CJF sources are either quasars or blazars, detectable in all wavebands of the electromagnetic spectrum accessible for astrophysical investigations. Their flux density is variable on a wide range of time-scales in all energy bands, and the events at the shortest timescales have not yet been resolved (Wagner & Witzel 1995 and references therein). A number of highly compact sources (all members of the CJF) show flux density changes within two hours (Witzel et al. 1986; Wagner & Witzel 1995 and references therein). Based on the CJF, we can perform a check of the radio flux variability, and find which part of the source — jet or core — contributes predominantly to the variability. We find evidence that suggests that BL Lac objects show the highest core+jet variability (25 ± 14 %), the quasars show weaker variability ($19\pm10\%$), and the galaxies, as expected, are least variable sources. The core is the most variable component for all classes. In galaxies with total flux-density variability less than BL Lacs and quasars, the jet components contribute $49\pm22\%$ of the variability. In quasars and BL Lacs — with higher total flux-density and flux-density variability — $36\pm17\%$ and $36\pm19\%$ of the variability, respectively, comes from the jet components.

5. Soft X-ray properties of the CJF sources

Many models accounting for the observed broadband spectra of blazars have been developed. Most of them attribute the emission at radio through optical wavelengths to synchrotron radiation, and X-ray through γ-ray emission to Compton scattering (e.g., Marscher 1980; Königl 1981; Sikora et al. 1994). The CJF sources have been observed within the ROSAT All-Sky survey and/or in pointed PSPC observations (Britzen et al. 2002b). Interestingly, most of the objects (the galaxies included) exhibit a nearly linear relation between X-ray and radio luminosities. Far above this general trend we find the three extreme BL Lac objects Mrk 421, Mrk 501 (each at low radio luminosities), and 3C 66A. The three Seyfert galaxies 2116+818, 0402+379, and 0309+411 also show excess X-ray emission at low radio luminosities. A similar behavior is seen in the plot of the X-ray vs. the optical luminosities.

5.1. Testing the beaming hypothesis

Comparing the observed and the predicted X-ray fluxes by assuming the observed X-rays to be of inverse Compton origin, we can compute the beaming or Doppler factor δ_{IC} for the CJF sources and can compare this Doppler factor with other beaming indicators derived from the VLBI observations, such as the value of the apparent expansion velocity.

The β_{app}-redshift distribution is different for the ROSAT detected and non-detected quasars. While the detected population shows more or less a constant β with redshift (from redshift 3 onwards the numbers are not significant due to lack of sources), the non-detected populations shows an increase in β_{app} with redshift. This will have to be investigated in more detail but might be evidence for the existence of two different populations of quasars.

The Doppler factors can be derived via the standard synchrotron self-Compton (SSC) argument, from equipartition arguments, and from the apparent velocities determined from VLBI observations. The comparison of Doppler factors calculated on the basis of velocity and X-ray information may answer the question whether the pattern and the bulk velocities are different. We find that apparent expansion speeds and Doppler factors have similar average numerical values. This can be taken as evidence that the bulk motion causing the beaming also causes the superluminal expansion, and that the existence of superluminal motion does not require different pattern and bulk velocities.

5.2. Correlation between X-ray prominence and large-scale radio structure

In Britzen et al. (2002b) we describe the VLA structure of the sources. The major part of the information on the large scale structure comes from VLA information by T. Pearson (http://www.astro.caltech.edu/tjp/cj/). VLA maps were not available for all sources and since the information on the extended structure has been collected from the literature, this data can not be homogeneous in quality. We find some evidence for an increase in the X-ray with increasing complexity of the extended radio structure for those sources detected by ROSAT. Except for two objects (0014+813, 1246+586), the point-like sources reveal relatively low X-ray fluxes. 101 of the 293 CJF sources reveal a point-like VLA structure. Among those, 71 have not been detected by ROSAT suggesting that X-ray selected samples preferentially have extended VLA structure.

References

Britzen, S. 2002, Reviews in Modern Astronomy, submitted

Britzen, S., R.C. Vermeulen, G.B. Taylor, et al. 2002a, in preparation

Britzen, S., W. Brinkmann, M. Gliozzi, et al. 2002b, in preparation

Cruddace, R.G., Hasinger, G.R., Schmitt, J.H. 1988, in ESO Conf. Proc. No. 28, Proc. of the Workshop: Astronomy from large data bases, ed. Murtagh F., Heck A., 177

Gregory, P.C. & Condon, J.J. 1991, ApJS, 75, 1011

Königl, A. 1981, ApJ, 243, 700

Kühr, H., Witzel, A., Pauliny-Toth, I. I. K., Nauber, U. 1981, A&AS, 45, 367

Marscher, A.P. 1980, ApJ, 235, 386

Sikora, M., Begelman, M.C., Rees, M.J. 1994, ApJ, 421, 153

Stickel, M. & Kühr, H. 1994, A&AS, 103, 349

Stickel, M., Meisenheimer, K., Kuehr, H. 1994, A&AS, 105, 211

Taylor, G.B., Vermeulen, R.C., Readhead, A.C.S., et al. 1996, ApJS, 107, 37

Vermeulen, R.C. & Taylor, G.B. 1995, AJ, 109, 1983

Vermeulen, R.C., Taylor, G. B., Readhead, A.C.S., Browne, I.W.A. 1996, AJ, 111, 1013

Wagner, S.J. & Witzel, A. 1995, ARA&A, 33, 163

Witzel, A., Heeschen, D.S., Schalinski, C.J., Krichbaum, T.P. 1986, Mitt.Astron.Ges., 65, 239

White, R.L. & Becker, R.H. 1992, ApJS, 79, 331

Xu, W., Lawrence, C.R., Readhead, A.C.S., Pearson, T.J. 1994, AJ, 108, 395

Zimmermann H.U., Becker W., Belloni T., et al. 1994, MPE Report, 257